NIH Public Access
Author Manuscript
Biochim Biophys Acta. Author manuscript; available in PMC 2009 December 1.

Published in final edited form as:
Biochim Biophys Acta. 2008 December ; 1778(12): 2814–2822. doi:10.1016/j.bbamem.2008.08.017.

The Antimicrobial Peptide Gramicidin S Permeabilizes Phospholipid Bilayer Membranes Without Forming Discrete Ion Channels

Md. Ashrafuzzaman[1,2], **O. S. Andersen**[2], and **R. N. McElhaney**[1]

1*Department of Biochemistry, University of Alberta, Edmonton, Alberta, Canada T6G 2H7*

2*Department of Physiology and Biophysics, Weill Medical College of Cornell University, New York, NY 10021, USA*

Abstract

We examined the permeabilization of lipid bilayers by the *β*-sheet, cyclic antimicrobial decapeptide gramicidin S (GS) in phospholipid bilayers formed either by mixtures of zwitterionic diphytanoylphosphatidylcholine and anionic diphytanoylphosphatidylglycerol or by single zwitterionic unsaturated phosphatidylcholines having various hydrocarbon chain lengths, with and without cholesterol. In the zwitterionic bilayers formed by the phosphatidylcholines, without or with cholesterol, the peptide concentrations and membrane potentials required to initiate membrane permeabilization vary little as function of bilayer thickness and cholesterol content. In all the systems tested, the GS-induced transient ion conductance events exhibit a broad range of conductances, which are little affected by the bilayer composition or thickness. In the zwitterionic phosphatidylcholine bilayers, the effect of GS does not depend on the polarity of the transmembrane potential; however, in bilayers formed from mixtures of phosphatidylcholines and anionic phospholipids, the polarity of the transmembrane potential becomes important, with the GS-induced conductance events being much more frequent when the GS-containing solution is positive relative to the GS-free solution. Overall, these results suggest that GS does not form discrete, well-defined, channel-like structures in phospholipid bilayers, but rather induces a wide variety of transient, differently sized defects which serve to compromise the bilayer barrier properties for small electrolytes.

Keywords

gramicidin S; antimicrobial peptides; lipid bilayer membranes; ion channels; membrane conductance; membrane defects

Introduction

The number of bacteria species that are developing resistance to conventional small molecule antibiotics is rising, which is becoming an increasingly serious public health problem (1,2). At the same time, the number of new antibiotics being developed, particularly those with novel

Address correspondence to: Md. Ashrafuzzaman, D.Sc., Department of Biochemistry, University of Alberta, Edmonton, Alberta, Canada T6G 2H7, E-mail: ashrafuz@ualberta.ca, Tel: 780 492 7469, Fax: 780 492 0886.

Publisher's Disclaimer: This is a PDF file of an unedited manuscript that has been accepted for publication. As a service to our customers we are providing this early version of the manuscript. The manuscript will undergo copyediting, typesetting, and review of the resulting proof before it is published in its final citable form. Please note that during the production process errors may be discovered which could affect the content, and all legal disclaimers that apply to the journal pertain.

NIH-PA Author Manuscript
NIH-PA Author Manuscript
NIH-PA Author Manuscript

NIH-PA Author Manuscript

NIH-PA Author Manuscript

NIH-PA Author Manuscript

mechanisms of action, has been limited. These developments have raised the specter of a possible “post-antibiotic era”, where seemingly minor bacterial infections could turn serious and even lethal due to a lack of effective drugs with which to treat them.

One approach to overcoming the bacterial drug resistance problem is to utilize naturally occurring antimicrobial peptides (AMPs) or their synthetic analogues to combat bacterial or fungal infections (see 3–5). Such peptides are produced by microorganisms to inhibit the growth of competitors or by plants and animals as part of their innate immune systems, and many of these AMPs are active against bacteria and fungi that are resistant to conventional antibiotics. AMPs exist in a wide variety of structural motifs (α-helical, *β*-sheet, linear and cyclic), but almost all are cationic amphiphiles that can interact with the bacterial inner membrane, which appears to be their primary target (6,7). The mode of action of AMPs is thought to involve an initial interaction between anionic phospholipids in the outer leaflet of the bacterial plasma membrane and the cationic amino acid residues of the peptide, followed by partial penetration of the hydrophobic amino acid residues of the peptide into the lipid bilayer. This peptide insertion somehow destabilizes the bilayer, and most AMPs are proposed to kill bacteria by disrupting the structural integrity of the plasma membrane phospholipid bilayer, which increases their non-selective permeability to ions and small molecules and thereby collapses the transmembrane potential, leading to cell de-energization and eventual death (5–7).

Gramicidin S (GS) is a cationic cyclic decapeptide with primary structure cyclo-(Val-Orn-Leu-$_{D}$-Phe-Pro)$_2$, which is secreted by the bacterium *Bacillus brevis* (8). GS is a potent antimicrobial agent at μM concentrations, exhibiting high killing activity against a broad spectrum of both Gram-positive and Gram-negative bacteria and pathogenic fungi (9,10). GS also exhibits appreciable hemolytic activity, which restricts its use as an antibiotic to topical applications. However, it is possible to design GS analogues with high antimicrobial activity but with markedly reduced hemolytic activity by altering both GS ring size and the enantiomeric conformation of key amino acid residues (11–14). Moreover, by designing GS analogs with augmented binding to anionic phospholipid and reduced binding to cholesterol-containing phospholipid bilayers, lipid specificity can be utilized to produce analogs with stronger antimicrobial and weaker hemolytic activities, thereby markedly increasing their therapeutic indexes (11-18). It is thus possible that GS analogs can be developed for use as oral or injectable broad-spectrum antibiotics for the treatment of infections caused by bacteria resistant to conventional antibiotics (see ref 5).

The three-dimensional structure of GS (Figure 1) has been studied using a wide range of physical techniques (see 9,10). In the minimum energy configuration shown in Fig. 1, the two Val-Orn-Leu sequences form an antiparallel *β*-sheet terminated by a Type II′ *β*-turn formed by the two $_{D}$-Phe-Pro sequences. This rather rigid structure is stabilized by four hydrogen bonds between the amide protons and carbonyl groups of the two Leu and two Val residues. GS is amphiphilic, having the two charged and somewhat polar Orn and the two $_{D}$-Phe side chains projecting from one side of the molecule and the four hydrophobic Val and Leu side chains projecting from the other. This overall conformation is maintained in water, in protic and aprotic organic solvents of varying polarity, and in detergent micelles and phospholipid bilayers. However, a recent study has suggested that GS may undergo a change from a more compact to a more extended *β*-sheet, *β*-turn conformation upon binding to phospholipid vesicles (15).

Considerable evidence has accumulated that the major target of GS is the lipid bilayer of bacterial or eukaryote membranes, and that the GS kills bacteria by somehow permeabilizing their inner membranes (see 2,3,16,17). Indeed, GS and its analogs have been shown to permeabilize various model lipid bilayer membranes (see 16,17). To determine the mechanism

NIH-PA Author Manuscript

NIH-PA Author Manuscript

NIH-PA Author Manuscript

underlying this permeabilization, a number of biophysical studies of GS interaction with lipid bilayer model membranes have been carried out (see 16,17). Differential scanning calorimetry studies show that GS more strongly perturbs the thermotropic phase behavior of anionic as compared to zwitterionic phospholipid bilayers and of more fluid as compared to less fluid bilayers (18). Densitometry and sound velocity studies show that GS decreases the density and volume compressibility of the host phospholipid bilayer by increasing the conformational disorder and motional freedom of the phospholipid hydrocarbon chains (19). ^{31}P nuclear magnetic resonance (NMR) (20) and X-ray diffraction (21) studies show that GS at lower concentrations causes thinning of phospholipid bilayers and induces the formation of inverted, nonlamellar cubic phases in phospholipid dispersions at higher concentrations. Fourier transform infrared spectroscopy studies show that GS is located in the interfacial region of phospholipid bilayers, and that it penetrates more deeply into anionic and more fluid bilayers (22). The presence of cholesterol attenuates all of the above effects of GS on phospholipid bilayers, at least in part by reducing the penetration of the peptide into the bilayer (22,23). Finally, solid-state ^{19}F-NMR studies on a ^{19}F-labeled GS analogue suggests that the GS molecule is aligned with its cyclic β-sheet lying flat in the plane of the bilayer, with its polar and positively charged Orn residues projecting toward the bilayer surface, where they can interact with negatively charged phosphate head groups of the phospholipid molecules, whereas the four hydrophobic Val and Leu residues project toward the bilayer center, where they interact with the phospholipid hydrocarbon chains (24).

Although these and other previous studies provide considerable insight into the interaction of GS with a variety of model and biological membranes, it remains unclear whether or not GS, like some α-helical antimicrobial peptides, forms well-defined, discrete ion-conducting channels in phospholipid bilayers. Though channel-like activity was reported in two previous studies of the effect of GS on planar lipid bilayers (25,26), the reported current events tend to be quite variable and other considerations would argue against GS being able to form a classical protein-lined channel (see 15-17). We therefore reinvestigated this question using black lipid membranes to assess whether GS forms discrete ion channels in phospholipid bilayers. Our results show that GS does not form structurally well-defined ion channels, but rather permeabilizes phospholipid bilayers by forming a wide variety of transient and variably-sized defects, with properties that depend only modestly on the head group composition and thickness of the host membrane. These defects are formed at peptide concentrations far below those required to rupture the phospholipid bilayers. That is, GS has profound effects on the barrier properties of lipid bilayers but does not appear to form discrete, peptide-induced ion channels. Our present findings provide another mechanism by which GS (and other AMPs) can exert its (their) antimicrobial action(s).

Materials and Methods

Materials

1,2-Dioleoyl-*sn*-glycero-3-phosphocholine ($DC_{18:1}PC$), 1,2-diecosenoyl-*sn*-glycero-3-phosphocholine ($DC_{20:1}PC$), 1,2-dierucoyl-*sn*-glycero-3-phosphocholine ($DC_{22:1}PC$), 1,2-diphytanoyl-*sn*-glycero-3-phosphocholine (DPhPC), 1,2-diphytanoyl-*sn*-glycero-3-[phospho-*rac*-(1-glycerol)] (sodium salt) (DPhPG) and cholesterol were from Avanti Polar Lipids (Alabaster, AL, USA); they were used without further purification. *n*-Decane was 99.9% pure from ChemSampCo (Trenton, NJ, USA). Squalene from Sigma (St. Louis, MO, USA) was filtered through chromatographic alumina (acid type from Sigma) to remove reactive species. GS was obtained from Sigma. Alamethicin from *Tricoderma viride*, was from Sigma. Gramicidin A analogue with 15 amino acids in the sequence (f-A-G-A-L-A-V-V-V-W-L-W-L-W-L-W-ea; Single-letter amino acid code; D-residues underlined; f, formyl; ea,

NIH-PA Author Manuscript

NIH-PA Author Manuscript

NIH-PA Author Manuscript

ethanolamine) was a generous gift from Dr. Roger E Koeppe II and D.V. Greathouse, Arkansas University, Fayetteville, Arkansas.

Stock solutions of GS (200 μM), alamethicin (1 μM) and the gramicidin A analogue were prepared using dimethylsulfoxide (DMSO) (Burdick and Jackson, Muskegon, MI). The electrolyte solution was 1.0 M NaCl buffered with HEPES (N-2-hydroxyethylpiperazine-N′-2-ethanesulfonic acid) (pH 7.0), both from Sigma. Unbuffered 1.0 M KCl was used for a few experiments.

Methods

Planar lipid bilayers were formed from 2.5% w/v solutions of the phospholipids in *n*-decane or squalene across a 1.5 mm hole in a Teflon® partition separating the two electrolyte solutions, using the pipet method of Szabo et al. (28). All experiments were done at 25 ± 0.5 °C. Care was taken to minimize the total amount of lipid (and *n*-decane or squalene) that was added; the total volume of the lipid/*n*-decane or squalene solution usually was at least 1000-fold less than the volume of the aqueous solution.

In most experiments, GS was added to the *trans* side of the lipid bilayers; the *cis* side was the electrical ground. Some experiments with $DC_{18:1}PC$ bilayers were also done by adding GS to both the *trans* and *cis* sides of the bilayer, with no obvious differences in the effects of GS on the electrical behavior of the phospholipid bilayer. The aqueous GS concentration required to produce ion conductance events in the decane-containing membrane systems with different lipid compositions (Table 1) varies (range 0.1–10.0 μM) depending on the applied potential (range 50–300 mV). Note that these GS concentrations are far below the solubility limit of GS in water (about 4.6 mM) (29). For a given transmembrane potential, the GS concentration required to produce comparable ion conductance events varies little with the phospholipid bilayer composition.

Single-channel experiments were done using the bilayer-punch method (30) and a Dagan 3900A patch-clamp amplifier (Dagan Corp., Minneapolis, MN) with a 3910 bilayer-expander module. The current signal of experiments with GS and alamethicin was first filtered at 20 kHz and then digitally filtered at 8 kHz. The current signal of experiments with gramicidin A channels was filtered at 2 kHz, digitized at 20 kHz, and digitally filtered at 500. The data were then plotted using Origin 6.1 (OriginLab Corp., Northampton, MA). All of the current traces were recorded for a period of at least 1-3 minutes, which is sufficient time to accumulate enough data to enable a valid statistical analysis.

Results

Experiments on DPhPC+DPhPG bilayers

The initial experiments were done with lipid bilayers constructed from 20% anionic lipid (DPhPG) and 80% zwitterionic lipid (DPhPC) with 1.0 M KCl in the aqueous solution in order to investigate the possible formation of GS “channels” or “pores” inside lipid bilayers using a similar protocol to Wu et al. (26). The current traces presented in Figure 2 show that GS, at 0.1 – 1.0 μM aqueous concentration, induces ion conductance events at all membrane potentials tested (50-300 mV). The conductance events show a wide distribution of current amplitudes ranging over several hundred pA with a trend toward higher “current levels” at the higher transbilayer potentials (see Figure 2A). The consequent conductance shows a wide distribution of its values (see Figure 2C). Some events appear relatively well-defined, as illustrated in the lower trace in Fig. 2B, but that was the exception. The predominant pattern was that of brief current “spikes” of varying amplitudes, similar to the pattern reported by Wu et al. (26). The GS-induced conductance events therefore were characterized by the construction of all-point

NIH-PA Author Manuscript

NIH-PA Author Manuscript

NIH-PA Author Manuscript

histograms (Figure 2C), which allows for a comparison among different experiments and experimental conditions.

Though difficult to quantify, the appearance rate for the conductance events increases with increasing [GS]. In comparable experiments using an opposite polarity of the transbilayer potential, we observed only few GS-induced conductance events, as was previously reported by Wu et al. (26).

Experiments on phosphatidylcholine bilayers: effect of bilayer thickness

The results in Fig. 2 suggest that GS produces ill-defined bilayer "instabilities" rather than distinct, well-defined, channel-like events. To further explore the characteristics of these events, we did experiments using unsaturated phosphatidylcholine bilayers having different acyl chain lengths. The motivation for these experiments was that bilayer thickness has pronounced effects on channels formed by membrane-active peptides that form well-defined channels, such as alamethicin and gramicidin A (31,32), an effect that can be understood in terms of the hydrophobic coupling between the lipid bilayer and the bilayer-spanning channels. Given the structure of GS, it was not clear whether the GS-induced conductance events should exhibit a similar hydrophobic mismatch dependence.

Figs. 3-5 show that GS induces ion conductance events with a large range of conductances (Figs. 3C, 4C and 5C) in bilayers composed of phosphatidylcholines having acyl chains of different lengths ($DC_{18:1}PC$, $DC_{20:1}PC$, $DC_{22:1}PC$) at all transbilayer potentials tested (50-300 mV). The overall appearance of these events varies little with bilayer thickness. Given the irregularity of the conductance events, we cannot exclude minor effects due to changes in bilayer thickness, but any such effects are much less than has been reported for alamethicin (31) or gramicidin A (32-35). In all cases, the frequency of GS-induced ion conductance events increases with increasing transbilayer potential and increasing [GS].

Though the conductance events may appear to exhibit some clustering under certain conditions, the prevailing observation is that they have a broad distribution—with current steps ranging between a few and several hundred pAs—and the point count vs. conductance plots show a wide range of conductances (Figs. 3C, 4C and 5C). Surprisingly, given the results obtained with the net negatively charged PC/PG bilayers (Figure 2), we observe no obvious polarity of transmembrane potential dependence of the GS-induced conductance events in neutrally charged PC bilayers.

The variability in the GS-induced current events differs strikingly from the patterns observed with linear gramicidins (gramicidin A) and alamethicin. Fig. 6A shows two current traces recorded in $DC_{18:1}PC$/*n*-decane bilayers in the presence of gramicidin A and alamethicin in independent experiments. The gramicidin A current trace shows discrete transitions between a few current levels that differ by a fixed amount (3.26±0.07 pA), the current transition amplitude. The alamethicin current trace shows discrete transitions between different current levels 0^{th}, 1^{st}, 2^{nd}, 3^{rd} etc. at 30±1, 120±3, 256±5, and 406±7 pA etc. respectively through an alamethicin channel containing variable numbers of alamethicin monomers. All point conductance level histograms (Fig. 6B) constructed from both gramicidin A and alamethicin current traces (Fig. 6A) show discrete peaks representing discrete conductances in both types of channels. The contrast between the results obtained with GS and both gramicidin A and alamethicin channels is striking.

To evaluate more quantitatively the [GS] and voltage (*V*) dependence of the GS-induced permeabilization of phospholipid bilayers, we evaluated the GS-induced activity using the all-points histograms (Fig. 7). The aggregate GS activity increases as a function of both [GS] and *V*. The apparent saturation of the activity vs. [GS] relation (Fig. 7B) may indicate some

NIH-PA Author Manuscript

NIH-PA Author Manuscript

NIH-PA Author Manuscript

saturation in the adsorption of GS to the bilayer. We did not pursue this question further because the phospholipid bilayers studied became too conducting for accurate measurements at [GS] > 10 μM. However, the bilayers remain intact at [GS] as high as 100 μM. From the slope of the activity vs. [GS] curve (Fig 7B), we estimate the apparent molecularity to be ~2.

Cholesterol exerts little effect on the GS-induced conductance events

Because bacterial membranes are cholesterol-free, whereas mammalian plasma membranes have high cholesterol contents (23), and because cholesterol is well known to effect the fluidity and thickness of phospholipid bilayers (16,17), we examined the effect of cholesterol on the GS-induced conductance events (Fig. 8). Cholesterol had no obvious effect on the stability, conductance and appearance frequency of GS-induced ion conductance events. As in cholesterol-free lipid bilayers, the GS-induced conductance events show a broad range of conductances (Fig. 8C). The time-averaged GS activity appears to be less than was observed in cholesterol-free bilayers, consistent with that reported in previous biophysical studies of the effects of cholesterol (23,36), which indicates that cholesterol modestly attenuates the action of GS on phospholipid bilayers.

Effects of different hydrocarbons (n-decane or squalene) on the GS-induced permeabilization of phospholipid bilayers

We also examined whether the GS-induced conductance events show any dependence on the hydrocarbon utilized for phospholipid bilayer generation in experiments on lipid bilayers formed using squalene rather than *n*-decane. The primary structural effect of squalene on lipid bilayers is to reduce the thickness of these bilayers (37,38). However, this variation in hydrocarbon structure may affect many other membrane properties as well. The current traces in Figure 8 show that GS-induced ion conductance events in squalene-containing bilayers appear at about 10-fold lower [GS] than those needed in *n*-decane-containing bilayers (cf. Fig. 4), but that the pattern otherwise is similar to what was observed in the decane-containing bilayers.

Discussion

Our results show that GS can induce ion conductance events in a variety of phospholipid bilayer membranes at aqueous [GS] varying between 0.1 and 10.0 μM. The GS-induced conductance events exhibit great variability (Figs. 2-5), with little evidence for *bona fide* channels with well-defined properties, such as those formed by gramicidin A or alamethicin (39–44) (Fig. 6). This behavior is seen at least [GS] 100-fold less than required to disrupt these black lipid membranes, indicating that the bilayer permeability defects observed are not prelytic phenomena, but bona fide manifestations of GS action.

The induction of ion conduction by GS depends only weakly on the phospholipid or on the presence of cholesterol and, except in the case of the nominally hydrocarbon-free bilayers formed using squalene, the GS-induced ion conductance does not depend greatly on the thickness of bilayers (Figs. 3 – 5). These results contrast sharply with the behavior observed with alamethicin (31) or gramicidin A (32-35), where the channel activity is profoundly affected by changes in bilayer thickness. This result, taken together with the wide distribution of the conductance events, suggests that GS forms neither phospholipid-lined toroidal pores (26,45,46) nor peptide-lined barrel stave pores (47), but rather permeabilizes lipid bilayers by the induction of transient defects in the bilayer core. An increase in bilayer thickness would be expected to destabilize toroidal pores due to an increased hydrophobic channel-bilayer coupling, or should at least require considerably higher peptide concentrations to obtain comparable channel frequency, contrary to what we observe. This absence of discrete pore formation is not surprising, given the small size of the GS molecule and the strong like-charge

NIH-PA Author Manuscript

NIH-PA Author Manuscript

NIH-PA Author Manuscript

repulsion that would accompany the formation of an aggregated channel structure. Moreover, because GS does not grossly disrupt or lyse phospholipid bilayers at the [GS] employed here, GS is unlikely to act via a carpet or bilayer solubilization mechanism (c.f. 48,49). One can thus conclude that GS permeabilizes a variety of phospholipid bilayer membranes by inducing the formation of a heterogeneous population of "defects" that are little affected due to the changes in channel-bilayer hydrophobic mismatch rather than by forming pores.

Our results suggest that GS might exert its actions by a mechanism similar to the so-called in-plane diffusion model of Bechinger or similar models (48,49). In this model, the insertion of antimicrobial peptides into phospholipid bilayers disorders the hydrocarbons chains of adjacent phospholipid molecules, locally thinning the bilayer, leading to local disturbances in bilayer packing and increases in bilayer permeability. Such bilayer perturbation requires minimal peptide aggregation, which would be both entropically and electrically unfavorable—consistent with the low apparent molecularity of the GS-induced events (~2, cf. Fig. 7). Yet, these regions of instability may overlap due to the lateral diffusion of GS within the membrane, thereby producing transient "openings" of a variety of sizes. Such GS-induced bilayer destabilization would be expected to be enhanced with the insertion of additional peptide molecules and with increasing transmembrane potential, as is observed. Interestingly, Jelokhany-Niaraki et al. (15) recently suggested a similar mechanism of action, based on data on GS-phospholipid interactions obtained with a wide variety of biophysical techniques. However, they did not carry out any electrophysiological experiments, such as we have performed here, to directly confirm their model.

Previously Wu et al. (26) studied the effect of GS on lipid bilayers composed of the zwitterionic lipid DPhPC and the anionic lipid DPhPG (4:1 molar ratio), and observed GS-induced conductance events only when the GS-containing solution was positive. We observe similar results in DPhPC/DPhPG bilayers. But in bilayers formed from only PC, GS-induced conductance events were observed at both positive and negative potentials. The fact that GS permeabilizes zwitterionic PC membranes equivalently for both polarities of the transmembrane potential, but in the presence of anionic phospholipids the polarities of the transmembrane potential become extremely important, implies that the charged phospholipid headgroups modulate the effective membrane potential sensed by GS. This difference between PC/PG and PC bilayers suggests that GS, all other factors equal, would be more effective in permeabilizing bacterial membranes, which have anionic lipids in the outer leaflet of the plasma membrane, than mammalian membranes, which have primarily the zwitterionic lipids PC and sphingomyelin in the outer leaflet.

In conclusion, the effects of GS on lipid bilayers depend both qualitatively and quantitatively on the type and charge of the lipid and to a lesser extent on the presence of cholesterol, but is almost insensitive to bilayer thickness. The concentration- and voltage-dependent permeabilization of phospholipid bilayers by GS does not occur by the formation of discrete, long-lived, peptide-induced channel structures or by overt bilayer solubilization, but by the formation of a wide distribution of short-lived, GS-induced defects in the host phospholipid bilayer. As this membrane-permeabilizing effect of GS is involved in its antimicrobial activity *in vivo*, the qualitatively different effects observed in PC/PG bilayers, as compared to PC bilayers, may provide a basis for the rational design of suitable GS analogs.

Acknowledgements

R.N.M. acknowledges financial support from an operating grant from the Canadian Institutes of Health Research and O.S.A. acknowledges financial support from the National Institutes of Health, U.S.A (grant no. GM21342).

NIH-PA Author Manuscript

NIH-PA Author Manuscript

NIH-PA Author Manuscript

References

1. Lohner, K.; Staudegger, E. Are we on the threshold of the post-antibiotics era?. In: Lohner, K., editor. Development of Novel Antimicrobial Agents: Emerging Strategies. Horizon Scientific Press; Wymondham, U.K.: 2001. p. 149-165.
2. Hall, RM.; Collis, CM. Origins and evolution of antibiotic and multiple antibiotic resistance in bacteria. In: Lohner, K., editor. Development of Novel Antimicrobial Agents: Emerging Strategies. Horizon Scientific Press; Wymondham, U.K.: 2001. p. 1-15.
3. Grantz, T.; Lehrer, RI. Antimicrobial peptides in innate immunity. In: Lohner, K., editor. Development of Novel Antimicrobial Agents: Emerging Strategies. Horizon Scientific Press; Wymondham, U.K.: 2001. p. 139-147.
4. Zasloff, M. The commercial development of antimicrobial peptide Pexiganam. In: Lohner, K., editor. Development of Novel Antimicrobial Agents: Emerging Strategies. Horizon Scientific Press; Wymondham, U.K.: 2001. p. 261-271.
5. Lee DL, Hosges RS. Structure-activity relationships of *de novo* designed cyclic antimicrobial peptides based on gramicidin S. Biopolymers 2003;71:28–48. [PubMed: 12712499]
6. Epand RM, Vogel HJ. Diversity of antimicrobial peptides and their mechanisms of action. Biochim Biophys Acta 1999;1462:11–28. [PubMed: 10590300]
7. Sitaram N, Nagaraj R. Interaction of antimicrobial peptides with biological and model membranes: Structural and charge requirements for activity. Biochim Biophys Acta 1999;1462:29–54. [PubMed: 10590301]
8. Gauge GG, Brazhnikova MG. Gramicidin S and its use in the treatment of infected wounds. Nature 1944;154:703.
9. Izumiya, N.; Kato, T.; Aoyaga, H.; Waki, M.; Kondo, M. Synthetic Aspects of Biologically Active Cyclic Peptides: Gramicidin S and Tyrocidines. Halsted Press; New York: 1979.
10. Waki, M.; Izumiya, N. Recent advances in the biotechnology of β-lactams and microbial bioactive peptides. In: Kleinhaug, H.; van Dohren, H., editors. Biochemistry of Peptide Antibiotics. Walter de Gruyter Co.; Berlin: 1990. p. 205-240.
11. Kondejewski LH, Farmer SW, Wishart DS, Kay CM, Hancock REW, Hodges RH. Modulation of structure and antibacterial and hemolytic activity by ring size in cyclic gramicidin S analogs. J Biol Chem 1996;271:25261–25268. [PubMed: 8810288]
12. Kondjewski LH, Jelokhani-Niaraki M, Farmer SW, Lix B, Kay CM, Sykes BD, Hancock REW, Hodges RS. Dissociation of antimicrobial and hemolytic activities in cyclic peptide diastereomers by systematic alterations in amphipathicity. J Biol Chem 1999;274:13181–13192. [PubMed: 10224074]
13. Jelokhani-Niaraki M, Kondejewski LH, Farmer SW, Hancock REW, Kay CM, Hodges RS. Diastereoisomeric analogues of gramicidin S: Structure, biological activity, and interaction with lipid bilayers. Biochem J 2000;349:747–755. [PubMed: 10903135]
14. Kondjewski LH, Lee DL, Jelokhani-Niaraki M, Farmer SW, Hancock RE, Hodges RS. Optimization of microbial specificity in cyclic peptides by modulation of hydrophobicity within a defined structural framework. J Biol Chem 2002;277:67–74. [PubMed: 11682479]
15. Jelokhani-Niaraki M, Hodges RS, Meissner JE, Hassenstein UE, Wheaton L. Interaction of gramicidin S and its aromatic amino acid analogues with phospholipid membranes. Biophys J BioFAST: July 11, 2008. 200810.1529/biophysj.108.137471
16. Prenner EJ, Lewis RNAH, McElhaney RN. The interaction of the antimicrobial peptide gramicidin S with lipid bilayer and biological membranes. Biochim Biophys Acta 1999;1462:201–221. [PubMed: 10590309]
17. Prenner EJ, Lewis RNAH, McElhaney RN. Biophysical studies of the interaction of the antimicrobial peptide gramicidin S with lipid bilayer model and biological membranes. Phys Can 2004;60:121–129.
18. Prenner EJ, Lewis RNAH, Kondejewski LH, Hodges RS, McElhaney RN. Diffraction scanning calorimetry study of the effect of the antimicrobial peptide gramicidin S on the thermotropic phase behavior of phosphatidylcholine, phosphatidylethanolamine and phosphatidylglycerol bilayer membranes. Biochim Biophys Acta 2001;147:211–223.

NIH-PA Author Manuscript NIH-PA Author Manuscript NIH-PA Author Manuscript

19. Krivanek R, Rybar P, Prenner EJ, McElhaney RN, Hianik T. Interaction of the antimicrobial peptides gramicidin S with dimyristoylphosphatidylcholine membranes: A densitometry and sound velocity study. Biochim Biophys Acta 2001;1510:452–463. [PubMed: 11342179]
20. Prenner EJ, Lewis RNAH, Kondejewski LH, Hodges RS, McElhaney RN. Nonlamellar phases induced by the interaction of gramicidin S with lipid bilayers. A possible relationship to membrane-disrupting activity. Biochemistry 1997;36:7906–7916. [PubMed: 9201936]
21. Staudegger E, Prenner EJ, Kriechbaum M, Degovics G, Lewis RNAH, McElhaney RN, Lohner K. X-ray studies on the interaction of gramicidin S with microbial lipid extracts: Evidence for cubic phase formation. Biochim Biophys Acta 2000;1468:213–230. [PubMed: 11018666]
22. Lewis RNAH, Prenner EJ, Kondejewski LH, Flach CR, Mendelsohn R, Hodges RS, McElhaney RN. Fourier transform infrared spectroscopic studies of the interaction of the antimicrobial peptide gramicidin S with lipid micelles and with lipid monolayer and bilayer membranes. Biochemistry 1999;38:15193–15203. [PubMed: 10563802]
23. Prenner EJ, Lewis RNAH, Jelokhani-Niaraki M, Hodges RS, McElhaney RN. Cholesterol attenuates the interaction of antimicrobial peptide gramicidin S with phospholipid bilayer membranes. Biochim Biophys Acta 2001;1510:83–92. [PubMed: 11342149]
24. Salgado J, Grage SL, Kondejewski LH, Hodges RS, McElhaney RN, Ulrich AS. Membrane-bound structure and alignment of the antimicrobial β-sheet peptide gramicidin S derived from angular and distance constraints by solid-state ^{19}F NMR. J Biomol NMR 2001;21:191–208. [PubMed: 11775737]
25. Heitz F, Kaddari F, Van Nau N, Verdussi F, Seheno RH, Lazaro RL. Ionic pores formed by cyclic peptides. Biochimie 1989;71:71–76. [PubMed: 2470418]
26. Wu M, Maier E, Benz R, Hancock REW. Mechanism of interaction of different classes of cationic antimicrobial peptides with planar bilayers and with the cytoplasmic membrane of *Escherichia Coli*. Biochemistry 1999;38:7235–7242. [PubMed: 10353835]
27. Benz R, Frohlich O, Lauger P, Montal M. Electrical capacity of black lipid films and of lipid bilayers made from monolayers. Biochim Biophys Acta 1975;394:323–334. [PubMed: 1131368]
28. Szabo G, EisenMann G, Ciani S. The effects of the macrotetralide actin antibiotics on the electrical properties of phospholipid bilayer membranes. J of Membr Biol 1969;1:346–382.
29. Jelokhani-Niaraki M, Prenner EJ, Kondejewski LH, Kay CM, McElhaney RN, Hodges RS. Conformation and other biophysical properties of cyclic antimicrobial peptides in aqueous solutions. J Peptide Res 2001;58:293–306. [PubMed: 11606214]
30. Andersen OS. Ion movement through gramicidin A channels – Single-channel measurements at very high potentials. Biophys J 1983;41:119–133. [PubMed: 6188500]
31. Hall JE, Vodyanoy I, Balasubramanian TM, Marshall GR. Alamethicin. A rich model for channel behavior. Biophys J 1984;45(1):233–47. [PubMed: 6324906]
32. Kolb HA, Bamberg E. Influence of membrane thickness and ion concentration on the properties of the gramicidin a channel. Autocorrelation, spectral power density, relaxation and single-channel studies. Biochim Biophys Acta 1977;464(1):127–41. [PubMed: 64260]
33. Mobasherry N, Nielsen C, Andersen OS. The conformational preference of gramicidin channels is a function of lipid bilayer thickness. FEBS Lett 1997;412(1):15–20. [PubMed: 9257681]
34. Hwang TC, Koeppe RE II, Andersen OS. Genistein can modulate channel function by a phosphorylation-independent mechanism: importance of hydrophobic mismatch and bilayer mechanics. Biochemistry 2003;42(46):13646–58. [PubMed: 14622011]
35. Galbraith TP, Wallace BA. Phospholipid chain length alters the equilibrium between pore and channel forms of gramicidin. Faraday discussion 1998;111:159–64.
36. Abraham T, Lewis RNAH, Hodges RS, McElhaney RN. Isothermal titration calorimetry studies of the binding of the antimicrobial peptide gramicidin S to phospholipid bilayer membranes. Biochemistry 2005;44:11279–11285. [PubMed: 16101312]
37. Benz R, Fröhlich O, Läuger P, Montal M. Electrical capacity of black lipid films and of lipid bilayers made from monolayers. Biochim Biophys Acta 1975;394(3):323–34. [PubMed: 1131368]
38. White SH. Formation of “solvent free” black lipid bilayer membrane from glyceryl monooleate dispersed in squalene. Biophys J 1978;23:337–347. [PubMed: 698340]
39. Eisenberg M, Hall JE, Mead CA. The nature of the voltage-dependent conductance induced by alamethicin in black lipid membranes. J of Membr Biol 1973;14:143–176. [PubMed: 4774545]

NIH-PA Author Manuscript

NIH-PA Author Manuscript

NIH-PA Author Manuscript

40. Hall JE. Toward a moelular understanding of excitability: Alamethicin in black lipid films. Biophys J 1975;15:934–939. [PubMed: 1182267]

41. Kolb HA, Boheim G. Analysis of the multi-pore system of alamethicin in a lipid membrane. II. Autocorrelation analysis and power spectral density. J of Membr Biol 1978;38:151–191.

42. Latorre R, Alvarez R. Voltage-dependent channels in planar lipid bilayer membranes. Physiol Rev 1981;61:77–150. [PubMed: 6258181]

43. Vodyanoy I, Hall JE, Balasubramanina JM, Marshall GR. Two purified fractions of alamethicin have different conductance properties. Biochim Biophys Acta 1982;684:53–58.

44. Mak DO, Webb WW. Two classes of alamethicin transmembrane channels: Molecular models from single-channel properties. Biophys J 1995;69:2323–2336. [PubMed: 8599639]

45. Matsuzaki K, Mitani Y, Akada K, Murase O, Moneyama S, Zasloff M, Miyajima K. Mechanism of Synergism between antimicrobial peptides magainin 2 and PGLa. Biochemistry 1998;37:15144–15153. [PubMed: 9790678]

46. Campagna S, Saint N, Molle G, Aumelas A. Structure and mechanism of action of the antimicrobial peptide piscidin. Biochemistry 2007;46:1771–1778. [PubMed: 17253775]

47. He K, Ludtke SJ, Huang HW. Antimicrobial peptide pores in membranes detected by neutron in-plane scattering. Biochemistry 1995;36:15614–15618. [PubMed: 7495788]

48. Bechinger B. Structure and functions of channel-forming peptides: Magainins, Secropins, Melittin and Alamethicin. J Membr Bio 1997;156:197–211. [PubMed: 9096062]

49. Bechinger B. The structure, dynamics and orientation of antimicrobial peptides in membranes by multidimensional solid-state NMR spectroscopy. Biochim Biophys Acta 1999;1462:157–183. [PubMed: 10590307]

NIH-PA Author Manuscript

NIH-PA Author Manuscript

NIH-PA Author Manuscript

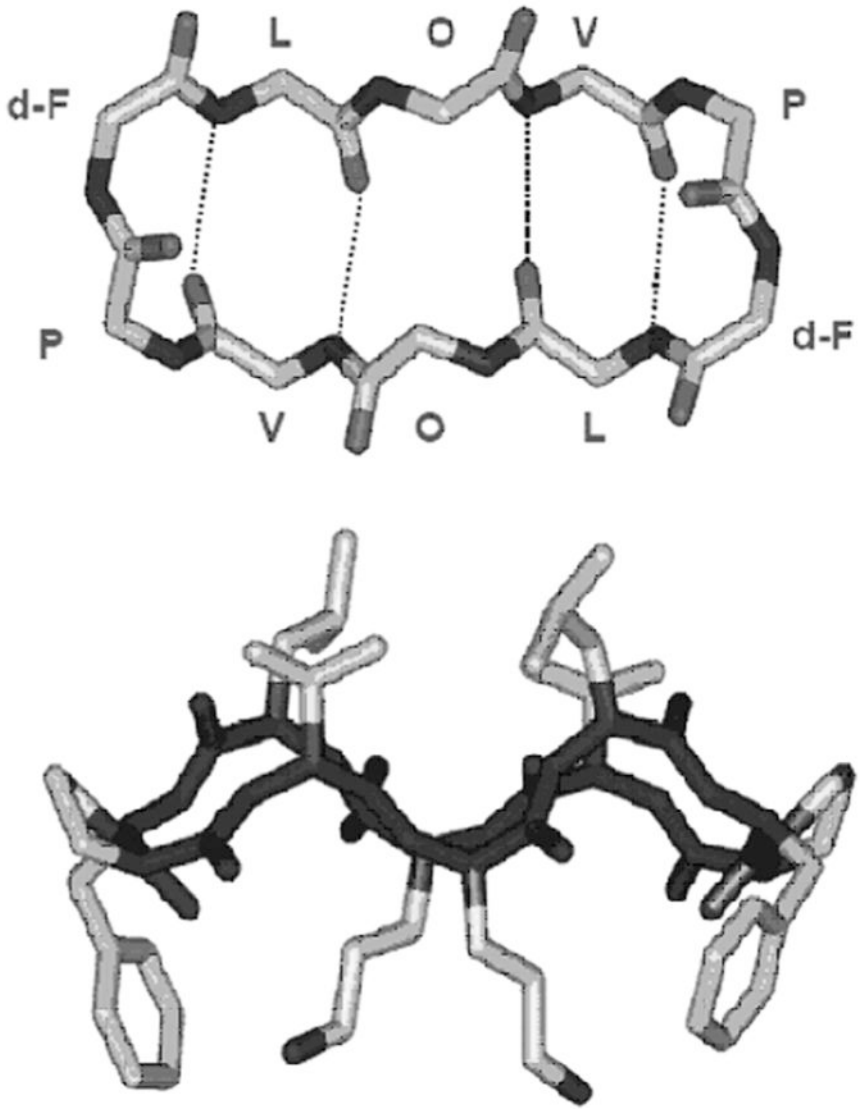

Figure 1.

Structure and conformation of GS. The top panel is a view of a GS molecule perpendicular to the plane of the ring, illustrating the peptide backbone structure and the positions of the hydrogen bonds in the antiparallel β-sheet region. The bottom panel is a view in the plane of the ring, indicating the spatial disposition of the hydrophobic Val and Leu residues (top) and the basic Orn residues (bottom) relative to the peptide ring.

NIH-PA Author Manuscript
NIH-PA Author Manuscript
NIH-PA Author Manuscript

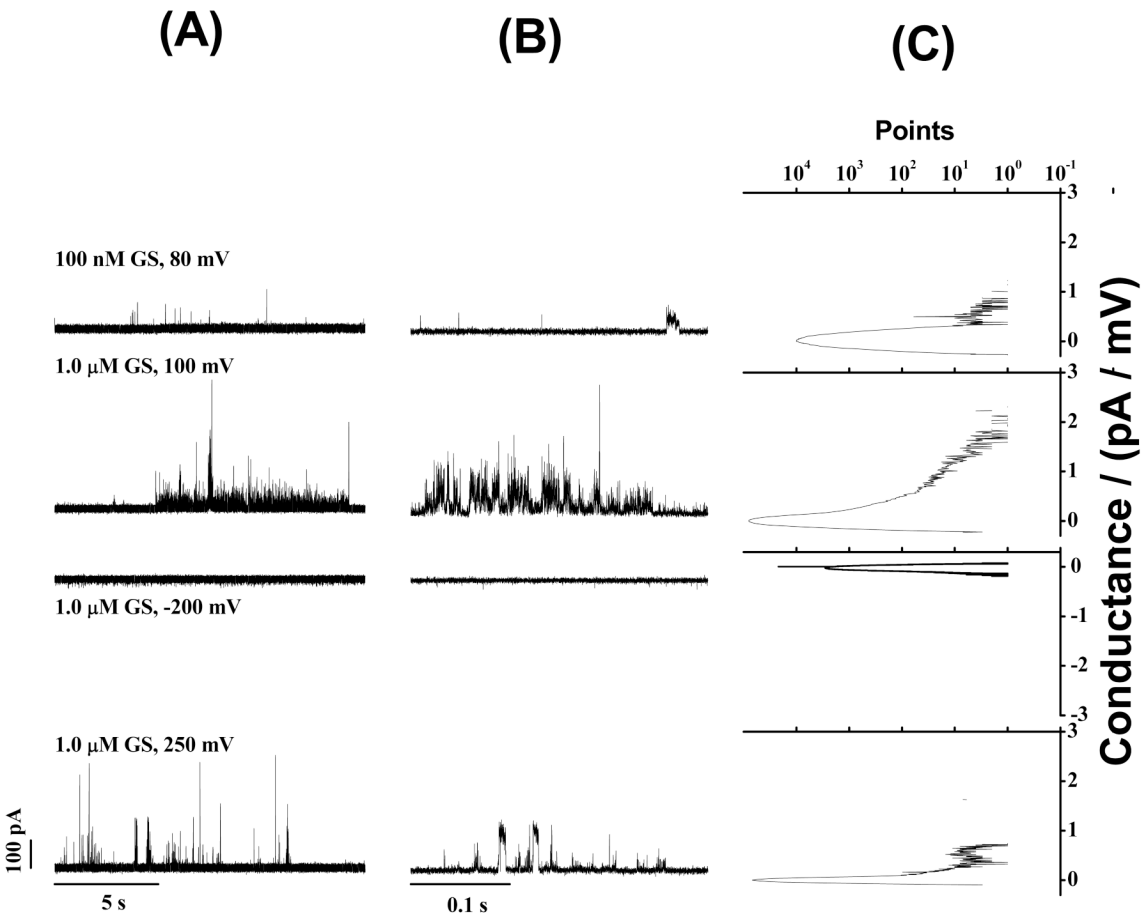

Figure 2.

GS-induced ion conductance events are observed at different transbilayer voltages (both positive and negative) in *n*-decane-containing lipid bilayers formed from a 4:1 mixture (molar) of DPhPC and DPhPG, the conditions used by Wu et al. (26). Both long-time (15 s) (A) and short-time (0.3 s) (B) current traces show current spikes due to the formations of GS-induced ion conductance events. (C) All point conductance level histograms constructed from the long-time traces (A). The peak at 0 pA/mV (Fig. 2C) represents the “unperturbed” bilayer (representing periods with no GS-induced conductance events). The traces were from independently prepared bilayers under the same experimental condition, using 1.0 M KCl (unbuffered).

NIH-PA Author Manuscript
NIH-PA Author Manuscript
NIH-PA Author Manuscript

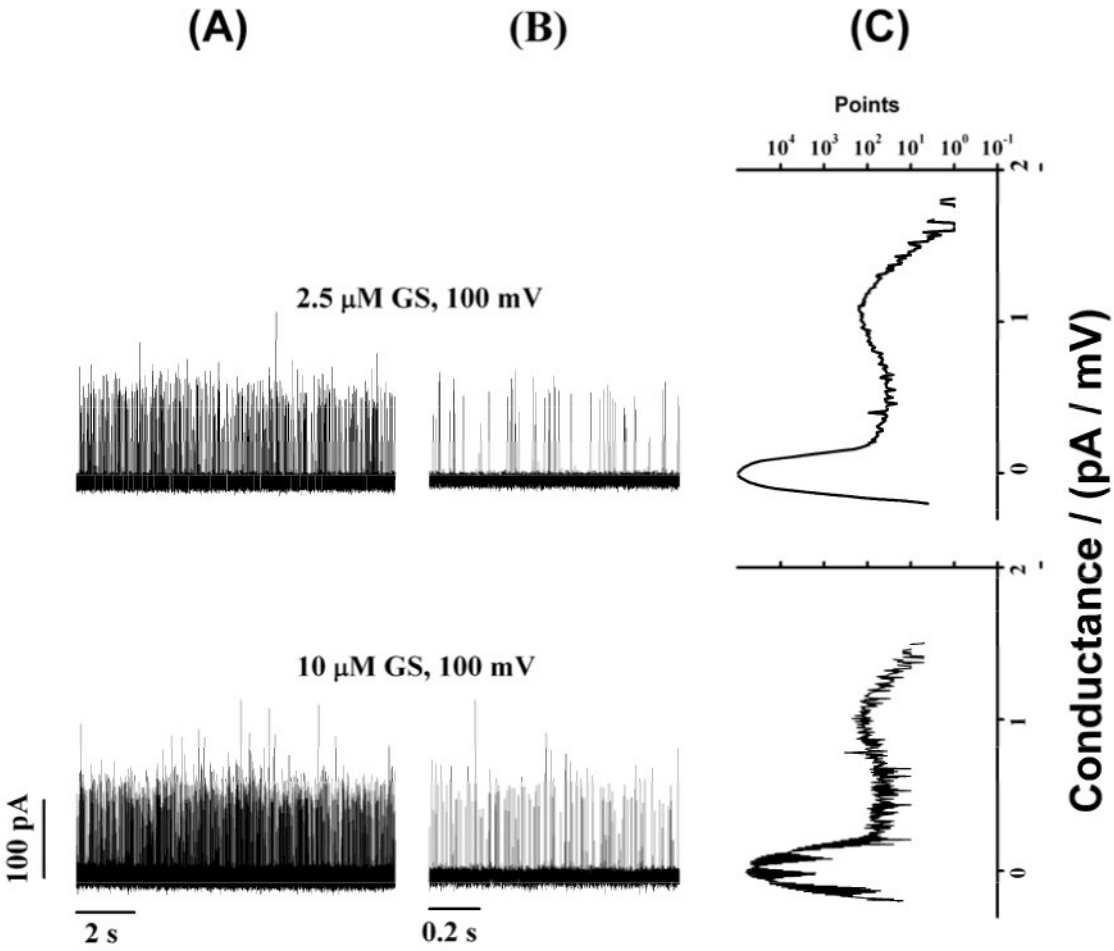

Figure 3.

GS-induced ion conductance events in zwitterionic phosphatidylcholine/*n*-decane bilayers at different [GS]. (A) and (B) show long-time (11 s) and short-time (1 s) current traces of GS-induced ion conductance events, respectively. (C) All point conductance level histograms constructed from the long-time traces (A). Two peaks (Fig. 3C) at 0 pA/mV and around 1 pA/mV respectively represent the baseline conductance of the "unperturbed" bilayer and the conductance levels of the GS-induced ion conductance events. $DC_{18:1}PC$/*n*-decane, 1.0 M NaCl, pH 7.0.

NIH-PA Author Manuscript
NIH-PA Author Manuscript
NIH-PA Author Manuscript

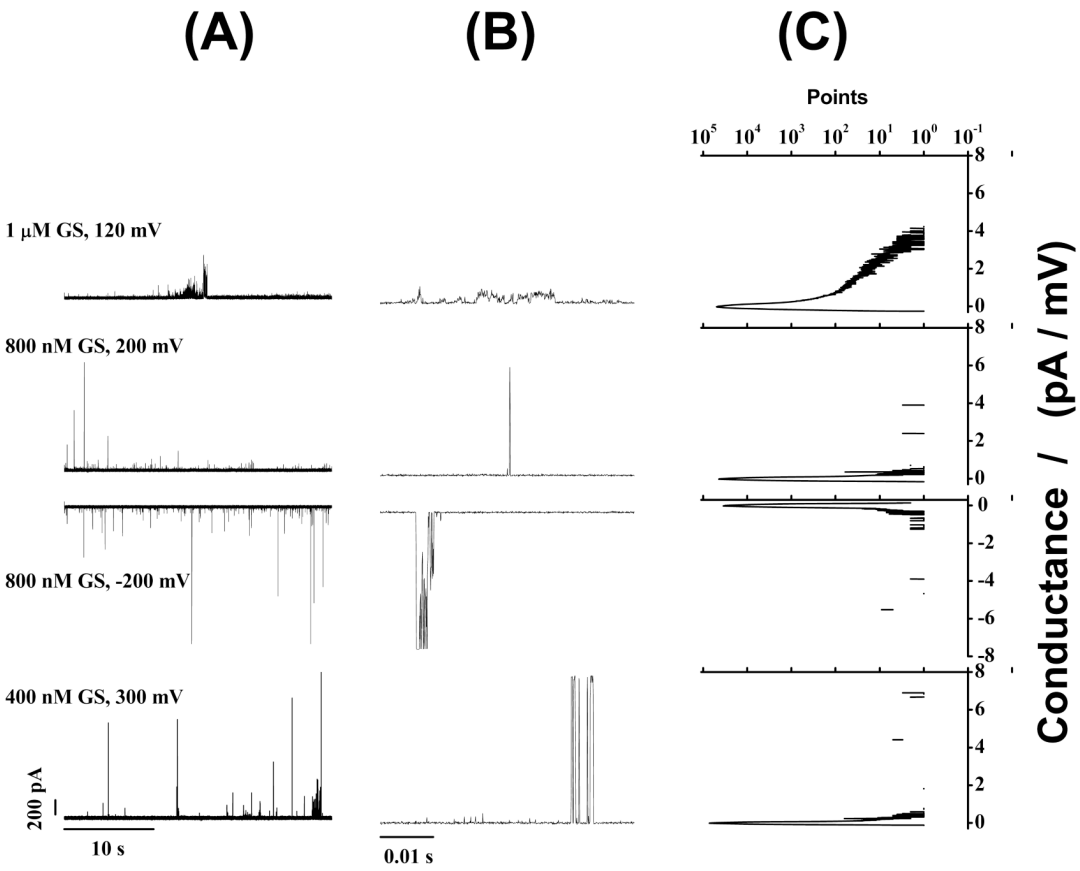

Figure 4.

GS-induced current events at different applied voltages (both positive and negative) in $DC_{20:1}PC$/*n*-decane bilayers. Both long-time (30 s) (A) and short-time (0.04 s) (B) records are shown. (C) All point conductance level histograms constructed from the long-time traces (A). GS-induced ion conductance events show a distribution of conductances (Fig. 4C)). 1.0 M NaCl, pH 7.0.

NIH-PA Author Manuscript

NIH-PA Author Manuscript

NIH-PA Author Manuscript

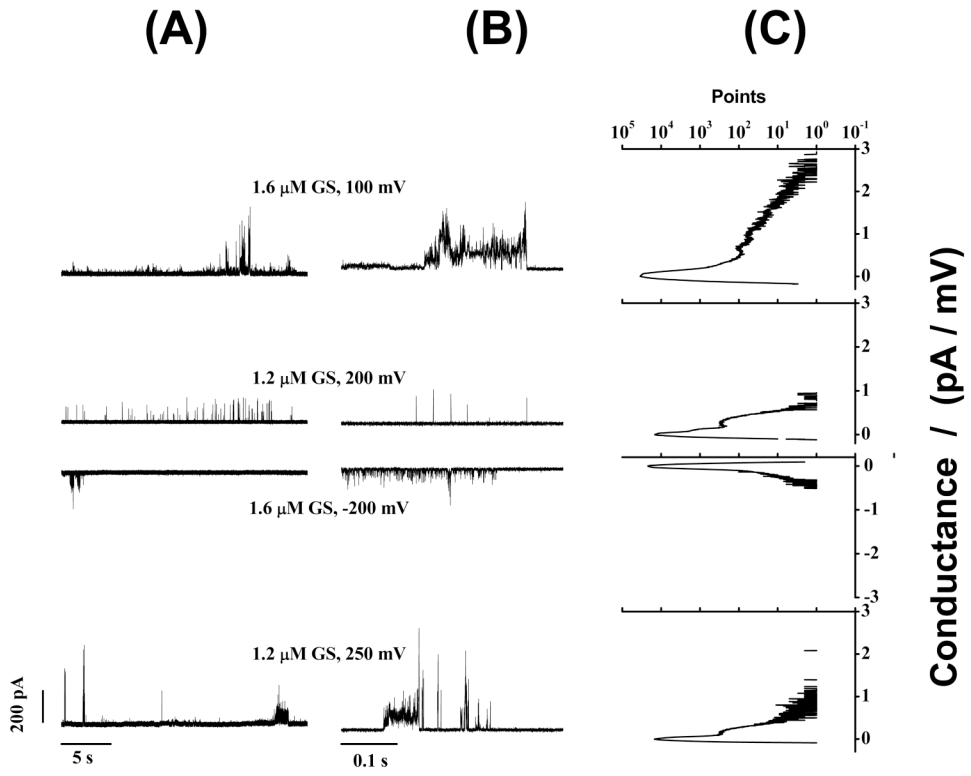

Figure 5.

GS-induced current events at different applied voltages (both positive and negative) in $DC_{22:1}PC$/*n*-decane bilayers. Both long-time (25 s) (A) and short-time (0.4 s) (B) records are shown. (C) All point conductance level histograms constructed from the long-time trace (A). GS-induced ion conductance events show a distribution of conductances (Fig. 5C). 1.0 M NaCl, pH 7.0.

NIH-PA Author Manuscript

NIH-PA Author Manuscript

NIH-PA Author Manuscript

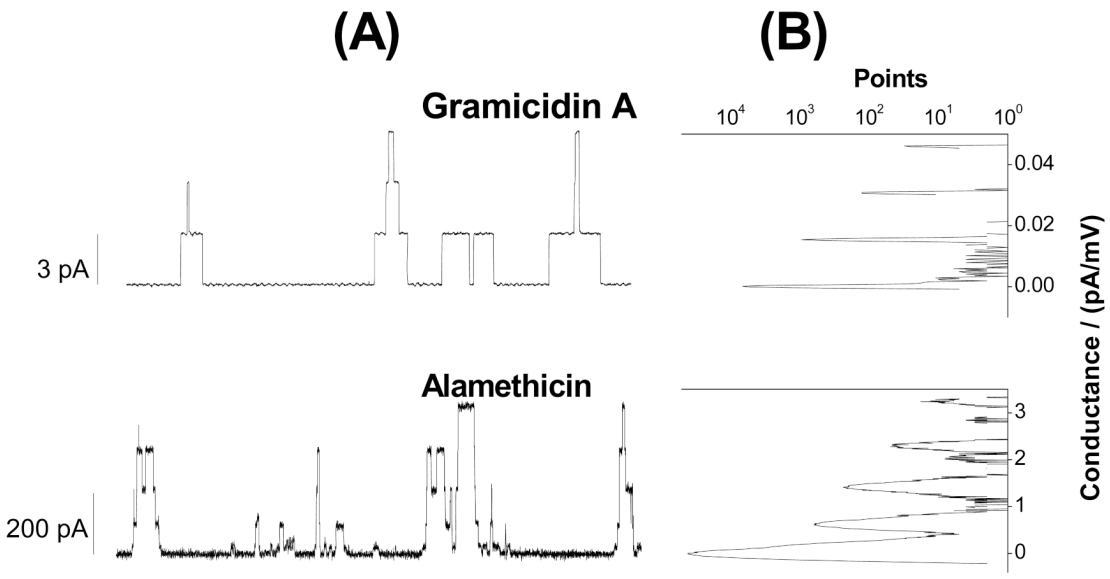

Figure 6.

Gramicidin A and alamethicin channel activity in $DC_{18:1}PC$/*n*-decane bilayers. A 10 s current trace (top panel of (A)) showing gramicidin A channel activity at 200 mV transmembrane potential. Multiple current levels are due to the presence of multiple gramicidin A channels at the same time. The current level transition for a gramicidin A channel is 3.26±0.07 pA. In the right top panel (B) all point conductance level histogram constructed from the current trace. Discrete conductance level shows that gramicidin A channel has constant conductance. Multiple discrete levels at equal current level intervals stand for the presence of multiple gramicidin A channels at same time. A 0.26 s current trace (bottom panel of A) showing alamethicin channel activity at 150 mV transmembrane potential. Multiple discrete current levels at 30±1, 120±3, 256±5, and 406±7 pA etc. represent 0, 1, 2, and 3rd etc. conductance levels through an alamethicin channel. Some current levels may also appear at values additive of few of those mentioned values for different discrete current levels due to the possible presence of multiple independent alamethicin channels. All point conductance level histogram constructed from the alamethicin current trace (in the right bottom panel (B)) shows discrete peaks representing discrete current levels in alamethicin channels. Like GS, alamethicin was added to the *trans* side of the lipid bilayer at ~10^{-8} M in the aqueous phase. The gramicidin A analogue was added to the both sides of the bilayer. In all cases, the aqueous phase contained 1.0 M NaCl, pH 7.0.

NIH-PA Author Manuscript

NIH-PA Author Manuscript

NIH-PA Author Manuscript

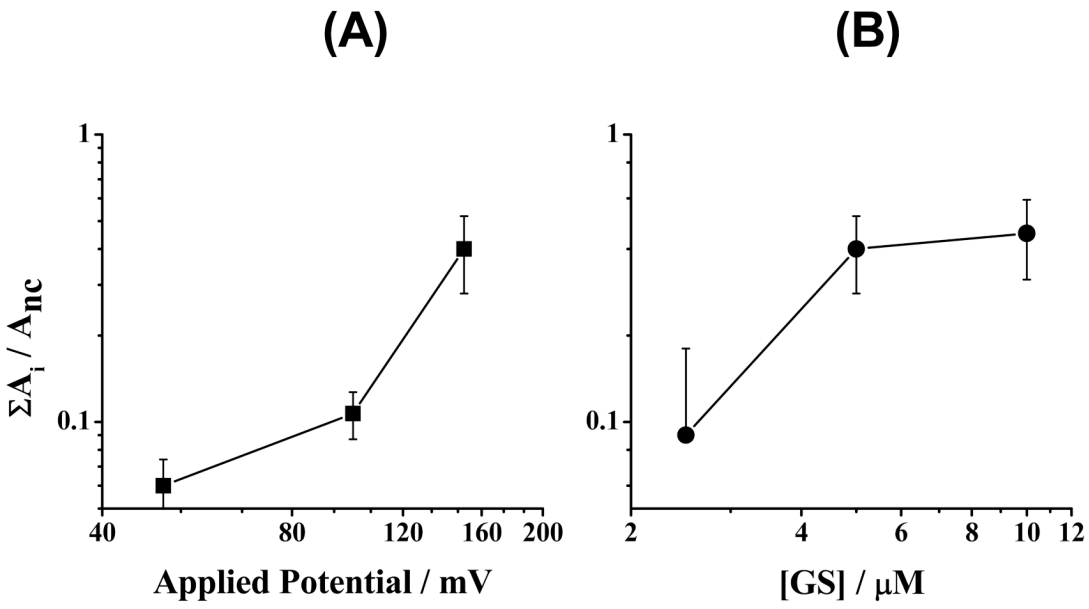

Figure 7.

Transmembrane potential- and [GS]-dependence of the GS-induced conductance events. $\Sigma A_i / A_{nc}$ (log-log plot) denotes the probability of observing all conductance events relative to the non-conductance events, which we define to be the GS-induced activity, where A_i and A_{nc} denotes the total point counts (areas under the peaks as shown in Figure 3C) at conductance level *i* (nonzero conductance) and non-conductance level (*nc*) meaning baseline (0 pA/mV conductance). The voltage effects are obtained from experiments with 5 μM GS. The [GS] effects are from experiments at 150 mV. $DC_{18:1}PC$/*n*-decane, 1.0 M NaCl, pH 7.0.

NIH-PA Author Manuscript
NIH-PA Author Manuscript
NIH-PA Author Manuscript

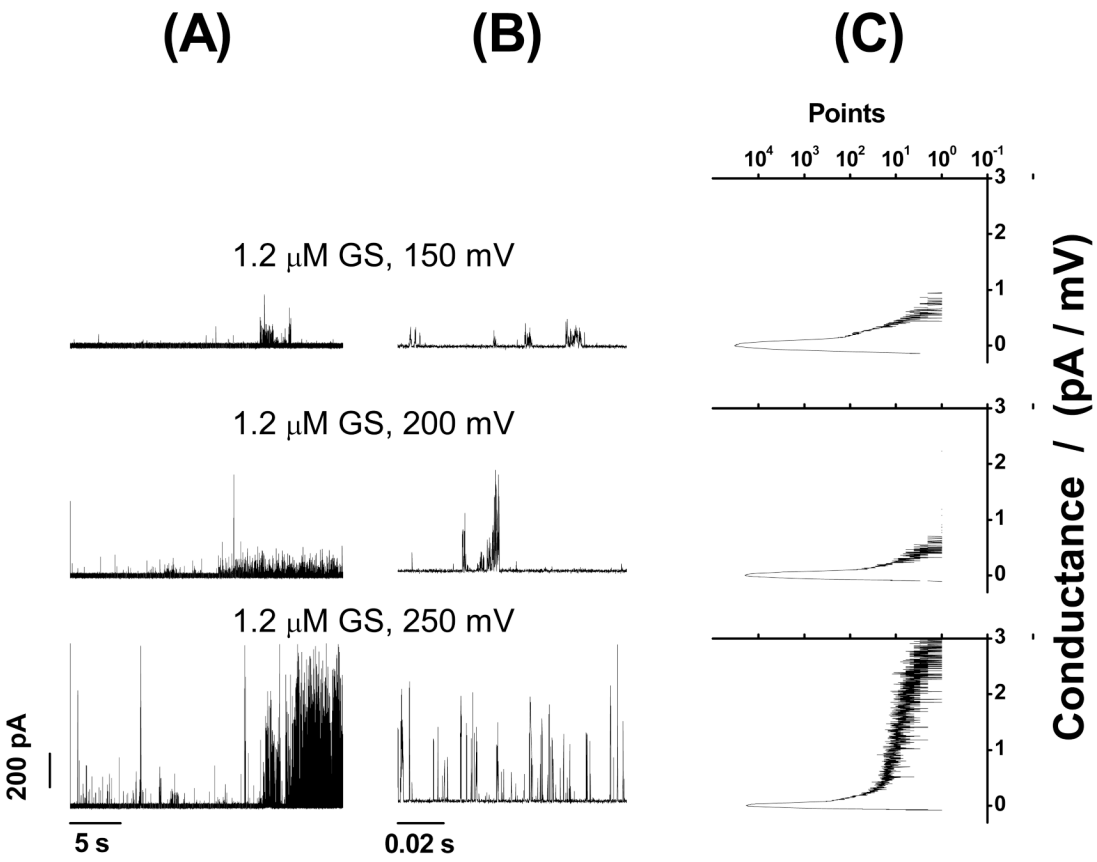

Figure 8.

GS-induced current events at different applied voltages in cholesterol-containing lipid bilayers. Both long-time (27 s) (A) and short-time (0.1 s) (B) records are shown. (C) All point conductance level histograms constructed from the long-time trace (A). GS-induced ion conductance events show a distribution of conductances (Fig. 8C). $DC_{18:1}PC$:cholesterol (1:1) in *n*-decane, 1.0 M NaCl, pH 7.0.

NIH-PA Author Manuscript

NIH-PA Author Manuscript

NIH-PA Author Manuscript

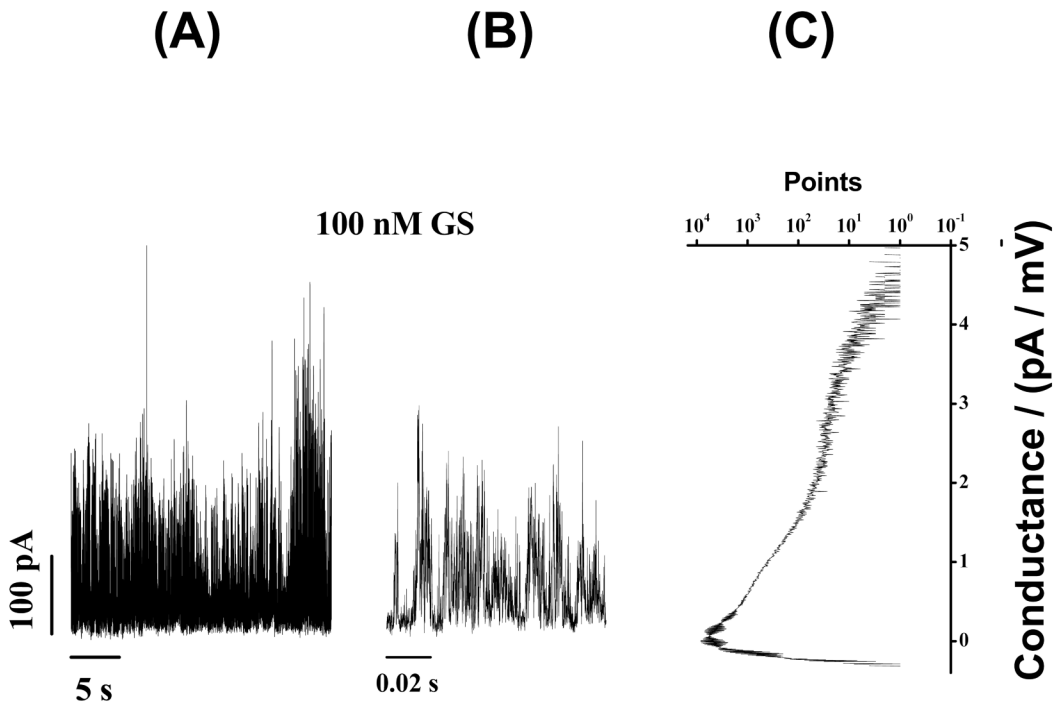

Figure 9.

GS-induced current events in squalene containing lipid bilayers. Both long-time (27 s) (A) and short-time (0.1 s) (B) records are shown. (C) All point conductance level histograms constructed from the long-time trace (A). GS-induced conductance events show a distribution of conductances (Fig. 9C). $DC_{20:1}PC$/squalene, 1.0 M NaCl, pH 7.0, 100 mV.

NIH-PA Author Manuscript

NIH-PA Author Manuscript

NIH-PA Author Manuscript

Table 1

Phospholipids and thicknesses

Phospholipid	Abbr.	Bilayer (with *n*-decane) thickness [a] / Å
1,2-Dioleoyl-*sn*-Glycero-3-Phosphocholine	$DC_{18:1}PC$	47.7±2.3
1,2-Diecosenoyl-*sn*-Glycero-3-Phosphocholine	$DC_{20:1}PC$	53.9±2.5
1,2-Dierucoyl-*sn*-Glycero-3-Phosphocholine	$DC_{22:1}PC$	58.4±2.5

[a](27)